Two-parameter monitoring in a lab-on-valve manifold, applied to intracellular H_2O_2 measurements†

Ilkka Lähdesmäki,*[a] Petr Chocholouš,‡[a] Andrea D. Carroll,[a] Judy Anderson,[b] Peter S. Rabinovitch[b] and Jaromir Ruzicka[a]

Received 9th December 2008, Accepted 14th April 2009
First published as an Advance Article on the web 27th April 2009
DOI: 10.1039/b822070k

This work introduces, for the first time, simultaneous monitoring of fluorescence and absorbance using Bead Injection in a Lab-on-valve format. The aim of the paper is to show that when the target species, cells immobilized on a stationary phase, are exposed to reagents under well-controlled reaction conditions, dual monitoring yields valuable information. The applicability of this technique is demonstrated by the development of a Bead Injection method for automated measurement of cell density and intracellular hydrogen peroxide.

Introduction

UV-VIS absorbance spectrophotometry and fluorescence spectrometry are widely-used detection techniques in biochemical research. Absorbance is mainly used for routine analyses, such as protein and DNA quantification, as well as enzymatic assays. Fluorescence, on the other hand, is used both for routine and cutting-edge applications and its use has experienced an explosive increase, especially in the field of cell biology. This is no doubt largely due to the significant progress made in fluorescent indicator technology during the last 15–20 years.[1,2]

Against this background, the combined monitoring of absorbance and fluorescence is desirable, as it will provide increased information content and, therefore, increased reliability of the results. For this reason, the two spectrometric modes were integrated into the micro Sequential Injection technique in the Lab-on-valve (LOV) format (for a description of the Lab-on-valve manifold, see refs 3 and 4). The versatility and usefulness of this novel tool are demonstrated in an automated method that allows intracellular H_2O_2 quantification and cell density measurement on the same sample. The method is built around the Bead Injection (BI) concept,[5] and implemented in an LOV fluidic manifold. Mouse embryonic fibroblasts, grown on Cytodex® microcarrier beads, are used as the target of the study. The cells are stained with a fluorescent H_2O_2 indicator and changes in intracellular H_2O_2 are elicited by exposing the cells to different levels of H_2O_2 in the extracellular medium. Absorbance measurements are used for quantification of cell density on the beads and are used to normalize the observed fluorescence response in three ways. The first correction involves normalizing the response to the cell density, the second and third corrections involve adjusting the response for attenuation by absorbance of excitation intensity and emission intensity, respectively.

Experimental

Microfluidic and spectrometric instrumentation

The experiments were carried out with a Sequential Injection apparatus, consisting of a FIAlab 3000 instrument (FIALab Instruments, Bellevue, WA, USA) with a Lab-on-valve (LOV) manifold mounted on the multiposition valve. The system is shown schematically in Fig. 1 (also see ESI†). In order to perform sensitive measurements in daylight conditions, a black opaque coating was applied to the LOV. A small clear area is left uncovered on the front face to allow visual inspection of the flow cell. A magnetic strip is attached to the opaque coating on the front face of the LOV, so that the clear area can be covered with another magnet when making measurements. The system was configured with a 1 mL syringe pump and a 1000 μL holding coil

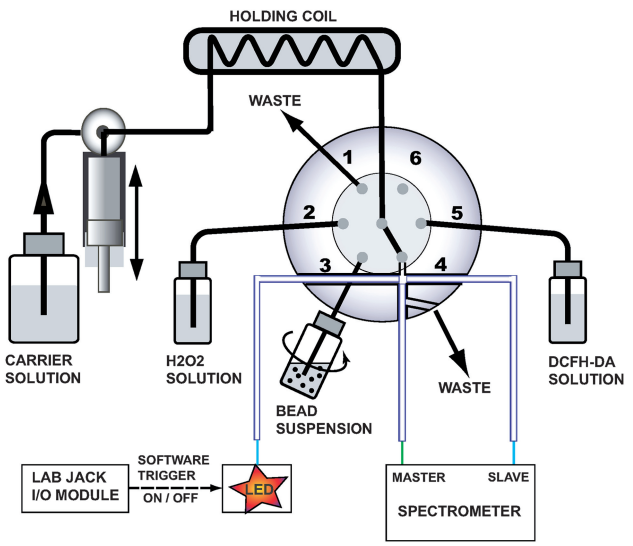

Fig. 1 A schematic view of the instrumental setup.

[a]*Department of Chemistry, University of Washington, Box 351700, Seattle, WA 98195-1700, USA*
[b]*Department of Pathology, University of Washington, Box 357470, Seattle, WA 98195-7705, USA*

† Electronic supplementary information (ESI) available: LOV photograph and software protocol. See DOI: 10.1039/b822070k

‡ Present address: Faculty of Pharmacy, Charles University, Heyrovského 1203, 500 05 Hradec Králové, Czech Republic.

made out of 1.6 mm/0.75 mm (o.d./i.d.) Teflon® tubing (Upchurch Scientific, Oak Harbor, WA, USA). The holding coil was covered with aluminium foil in order to protect light-sensitive reagents. The flow cell volume was approximately 5 μL.

A white XLamp LED (Super Bright LEDs, St. Louis, MO, USA) filtered with a 470/40 nm bandpass filter (Chroma Technology, Rockingham, VT, USA) was used as a light source. The light source power supply (fabricated in-house) was equipped with electronics to allow software control. The power supply was connected to a LabJack I/O module (LabJack Corporation, Lakewood, CO, USA) in order to enable the user to trigger the light source on and off from the FIALab software. An SD2000 dual sensor CCD spectrometer (Ocean Optics, Dunedin, FL, USA) was used for recording the absorbance and the fluorescence signals. Absorbance was recorded on the 'slave' spectrometer and fluorescence on the 'master' spectrometer. An optical fiber with a core diameter of 600 μm (CeramOptec, East Longmeadow, MA, USA) was used to direct light from the light source to the flow cell (fiber #1 in Fig. 2A). Light was collected from the flow cell and transmitted to the absorbance detector by a 400 μm fiber (fiber #3, from Ocean Optics), and to the fluorescence detector by a 600 μm fiber (fiber #2, from CeramOptec). The absorbance signal was monitored at 470 nm and the fluorescence signal was monitored at 530 nm.

Reagents

Unless otherwise noted, the chemicals were analytical-grade reagents from Sigma (St. Louis, MO, USA) or Mallinckrodt Baker (Phillipsburg, NJ, USA).

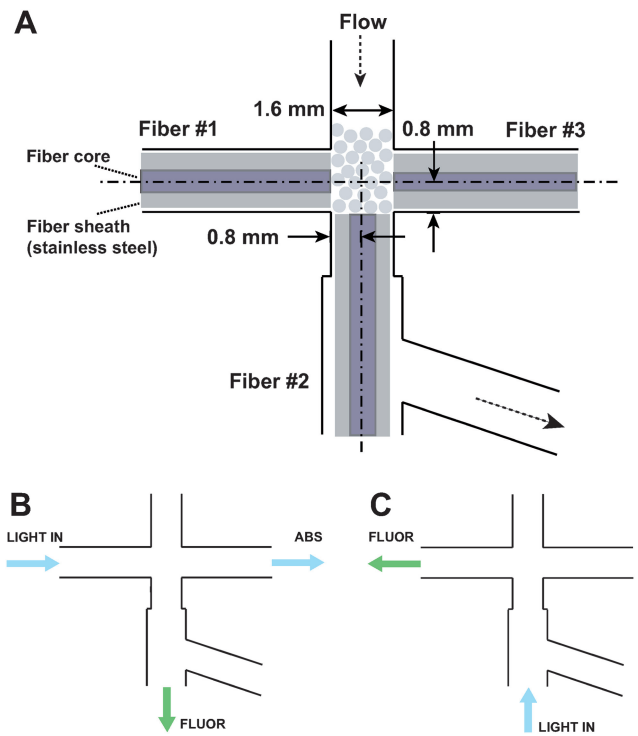

Fig. 2 (A) A close-up view of the flow cell. (B) The standard light path arrangement. (C) The light path arrangement for determining the emission path length.

Physiological buffer solution. A vial of Hanks Balanced Salt Solution (HBSS) powder (containing 137 mM NaCl, 5.4 mM KCl, 1.3 mM $CaCl_2$, 0.8 mM $MgSO_4$, 0.4 mM KH_2PO_4, 0.3 mM $NaHPO_4$ and 5.6 mM glucose after full dilution; Sigma H1387) was dissolved in 900 mL water. HEPES (Sigma H6147) was added to a final concentration of 10 mM and the pH adjusted to 7.4 with 1 M sodium hydroxide. Glucose was added to a final concentration of 4.6 g/L. The solution was then diluted to its final volume (1.0 L).

Carrier solution. Physiological buffer solution was used as the carrier solution.

Indicator solutions

Fluorescein solutions. For determining the effective excitation and emission path lengths, a stock solution of 10 mM sodium fluorescein (Sigma 28803) was made using the physiological buffer solution. Working solutions (1, 5, 10 and 20 μM) were prepared by further dilution with the physiological buffer solution.

Crystal violet solution. For manual cell counting, a stock solution of 0.5% (w/v) crystal violet (Sigma C3886) was made in methanol. The working solution was prepared by diluting the stock solution with 0.12 M citric acid to 0.12% (v/v).

DCFH-DA solution. For intracellular H_2O_2 measurements, a stock solution of 20 mM dichlorofluorescein diacetate (DCFH-DA, Sigma D6883) was prepared in dimethyl sulfoxide containing 10% Pluronic F-127 (a polyoxyethylene-type non-ionic detergent). An intermediate stock solution of 0.6 mM DCFH-DA was prepared by diluting with the physiological buffer solution. Fresh intermediate stock solution was made for each day of experiments and kept on ice. The working DCFH-DA solution was obtained by diluting the intermediate stock solution with the physiological buffer solution to 30 μM. A fresh vial of the working solution was prepared for each measurement cycle.

H_2O_2 solutions. An intermediate stock solution was prepared by diluting 30% H_2O_2 with the physiological buffer solution to a concentration of 20 mM. Working solutions of H_2O_2 were prepared by further dilution of the intermediate stock with the physiological buffer solution.

Bead suspension. Cytodex® microcarrier beads (Sigma C0646, empty or cell-bearing) were prepared for experiments by mixing 1 part of wet beads with 9 parts of Dulbecco's Modified Eagle Medium (DMEM, Cambrex BioScience, Walkersville, MA, USA) cell culture solution, resulting in a 10% (v/v) suspension.

Cell culture

Mouse embryonic fibroblasts were grown on Cytodex® microcarrier beads, in DMEM supplemented with glutamine, serum, penicillin/streptomycin and non-essential amino acids. For cell density calibration, 500 μL aliquots (wet volume) of Cytodex® beads were seeded with 1×10^6, 2×10^6, 4×10^6 and 8×10^6 cells. After adhesion and growth, this resulted in four populations expressing different cell densities. Bare Cytodex® beads

were used as a blank population. For intracellular H_2O_2 experiments, the cell culture process was identical, except that fewer seeding densities were used.

Determination of excitation and emission path lengths in the flow cell

A close-up view of the flow cell is presented in Fig. 2A. It shows the absorbance path length (1.6 mm), the excitation path length (the distance from the surface of the illuminating fiber to the volume of fluorescence interrogation, 0.8 mm) and the emission path length (the distance from the volume of fluorescence interrogation to the surface of the collection fiber, 0.8 mm). However, these geometric path lengths are only approximations that do not take into account light scattering by beads in the flow cell or off-center placement of fibers in their sheathing. A more accurate estimate can be obtained by experimental determination as shown below.

Excitation path length. The excitation path length was determined by packing Cytodex® beads in the flow cell, injecting a solution of fluorescein onto the column and measuring the resulting fluorescence and absorbance signals. Since the beads are positively charged and fluorescein is negatively charged, fluorescein will accumulate on the column. The process was carried out using fluorescein concentrations of 1, 5, 10 and 20 μM, resulting in a calibration curve (Fig. 3A). High fluorescein concentrations were purposely chosen to extend the measurements into the non-linear portion of the calibration curve. The non-linear behavior at high concentrations is due to attenuated excitation intensity, caused by the absorption of excitation light.

The calibration curve can be made linear by considering the attenuating effect of light absorption. Absorption attenuates the excitation intensity by a factor $10^{-l\_ex \cdot A}$, where A is the recorded absorbance signal. The term l_ex represents the relative length of the excitation light path, with respect to the absorbance path length. In other words, it is the ratio of the excitation path to the absorbance path. In order to restore the linearity of the fluorescence signal F, it needs to be divided by the attenuation factor:

$$F_{\text{lin}} = \frac{F}{10^{-l\_ex \cdot A}}$$

where F is the raw data response and F_{lin} is the linearized fluorescence response.

The above relationship can now be utilized to determine the effective excitation path length. This was done mathematically by varying the parameter l_ex and computing F_{lin} until a linear calibration curve was obtained. A linear curve was obtained with an l_ex value of 0.50, as illustrated in Fig. 3A. This effective path length agrees with the geometrically determined value of 0.8 mm/1.6 mm = 0.5. It should be mentioned that the fluorescence signal was measured at 540 nm, where fluorescein shows negligible absorbance. The reason for choosing this wavelength was to avoid distortions due to the inner filter effect, *i.e.* re-absorption of the emitted fluorescence.

Emission path length. To determine the emission path length, the light source was connected to fiber #2, and the fluorometric detector to fiber #1 (Fig. 2C). This reverses the excitation and emission paths, relative to the standard configuration seen in Fig. 2B, making l_ex a measure of what normally is the emission path. In this configuration, it is not possible to measure the absorbance signal. However, since the bead loading and fluorescein delivery processes are identical to those in the excitation path length experiments, the same absorbance values can be used. The experiments yield a path length value of 0.50 (Fig. 3B), which is again consistent with the geometric approximation of 0.8 mm/1.6 mm = 0.5. We will call this the effective emission path length (l_em) and will use it for evaluation of cellular responses to stimuli.

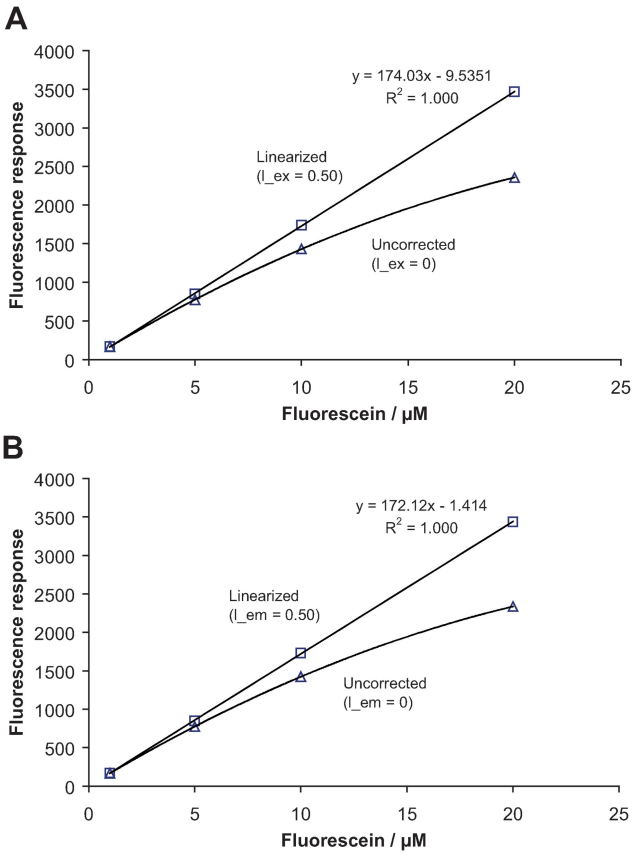

Fig. 3 (A) Determination of the excitation path length. (B) Determination of the emission path length. The data points represent averages of two measurements ($n = 2$). The original fluorescence signal is shown using triangles, with a second order polynomial fit through the points. The linearized signal is shown using squares, with a linear fit through the points.

Microfluidic protocol

The instrument was controlled by FIAlab for Windows software version 5.9.239. In general, the fluidic protocol was started by aspirating beads at 20 μL/s, delivering them to the flow cell at 10 μL/s and washing with the carrier solution. The absorbance signal was monitored throughout the delivery and wash process to obtain a signal for cell density, as well as to verify the reproducibility of packing the bead column. After packing and washing the column, 500 μL of a solution containing 30 μM dichlorofluorescein diacetate (DCFH-DA, an intracellular H_2O_2 indicator) was pulled into the holding coil. The solution was

slowly perfused over the bead column in an intermittent fashion (flow on 3 s, flow off 3 s) to stain the cells with DCFH-DA. The duration of the staining step was 5 min. After that, a 500 μL bolus of a H_2O_2 solution was pulled into the holding coil and subsequently delivered onto the bead column, followed by a wash with carrier solution. During the H_2O_2 delivery, the fluorescence signal was intermittently monitored by pulsing the light source (2 s on, 23 s off). Pulsed detection was necessary due to the light sensitivity of the DCFH indicator that would be oxidized by prolonged exposure to intense light. Finally, the bead column was removed by aspirating it back into the holding coil and discarding to waste. An overview of the fluidic protocol is shown in Table 1. The detailed FIAlab for Windows software script has been made available as electronic supplementary information (ESI).†

The choice of 5 min as the staining period duration warrants some further explanation. It has been shown that a period of 15 min is required to achieve equilibrium DCFH-DA concentration inside cells.[6] However, since the staining is done as part of the measurement cycle, using a period of 15 min would make the cycle prohibitively long. In preliminary experiments, 5 min was observed to result in sufficient loading of the dye and represents a compromise between stain intensity and experimental throughput.

Manual cell count

In order to count cell populations manually, the instrument was programmed to dispense a 240 μL aliquot of the bead suspension into a separate collection vial. The beads were washed with physiological buffer solution and allowed to settle. The supernatant was removed and the beads were suspended in 150 μL of 0.12% crystal violet in 0.12 M citric acid. The resulting suspension was mixed vigorously to extract the nuclei out of the cells, incubated 1 h at room temperature and mixed again. Finally, an aliquot of the supernatant was removed for counting on a hemacytometer counting chamber. The protocol is a modification of the method developed by Sanford *et al.*[7]

Results and discussion

Calibration of automated cell density determination

The absorbance of each bead/cell population was measured at 470 nm, as shown in the first part of the fluidic protocol in Table 1. An example of the absorbance signals is shown in Fig. 4A. A calibration scale for the absorbance values was created by manually counting the cell density in each of the populations, as described in the Experimental section. It was performed in quadruplicate for each cell population ($n = 4$).

Table 1 Fluidic protocol

Step	Description
1.	Reference absorbance signal in empty flow cell
2.	Load and wash bead column. While loading beads, record absorbance signal
3.	Prime DCFH-DA solution inlet
4.	Aspirate 500 μL DCFH-DA solution
5.	Stain cells by dispensing DCFH-DA solution onto bead column (intermittent flow: 3 s on, 3 s off)
6.	Prime H_2O_2 solution inlet
7.	Aspirate 500 μL H_2O_2 solution
8.	Deliver H_2O_2 solution onto bead column (5 μL/s). While delivering H_2O_2, pulse LED (2 s on, 23 s off). Record fluorescence signal when LED on
9.	Discard bead column

A mathematical relationship between the absorbance values and manual cell counts was established by subjecting the data to regression analysis (Fig. 4B). The signal is non-linear, which is typical behavior for transmission-type cell density probes.[8] The regression fit equation was $D = 565A^2 - 76.6A + 0.126$, where A is the absorbance value of the bead/cell column, and D is the manual cell density count (average number of nuclei counted per hemacytometer square). The correlation coefficient (R^2) was 0.999. The results show that the absorbance value correlates well with manual cell count, and can thus be used for determining the cell density on beads.

It should be noted that instead of pure absorbance, the cell density signal is likely to be a mixture of absorbance and forward scatter. Scattering is commonly utilized for measuring the density of bacterial and yeast cultures, and applications involving

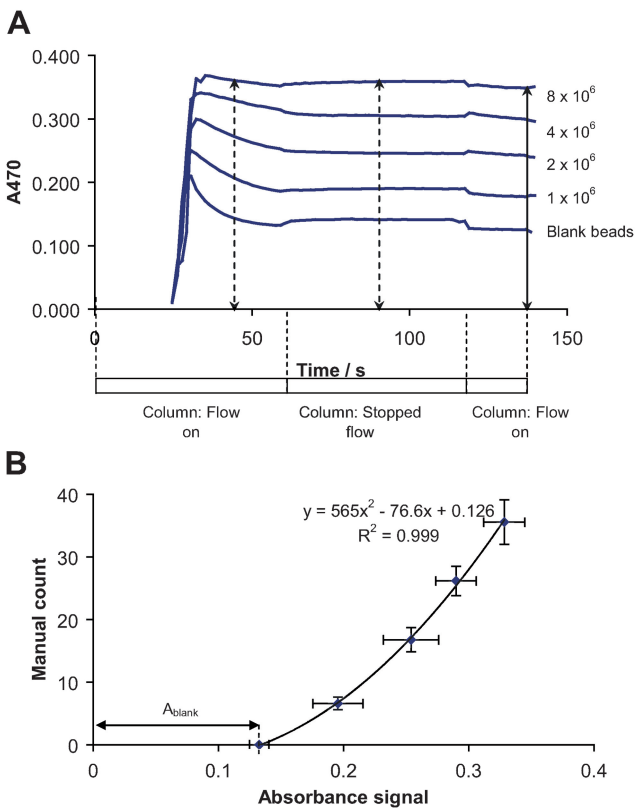

Fig. 4 (A) Absorbance signals for different cell densities. The labels on the right refer to the seeding densities of each population. The arrows indicate possible points for measuring the absorbance signal. The point on the left is not the best choice since the culture medium is still getting washed off the column. The middle point shows compromised reproducibility, since the flow is stopped and the bead column is expanding. The solid arrow represents the selected measurement point. (B) Calibration graph for cell density measurements. Manual count on the y-axis refers to the average number of cells counted in a hemacytometer square. A_{blank} denotes the absorbance of bare beads. The values were derived from four replicate measurements ($n = 4$).

mammalian cells have also been demonstrated. Connors and Heino have shown that side scatter caused by cells can be utilized to determine mammalian cell adhesion onto a bead substrate.[9] Wu *et al.* have evaluated several commercial scattering probe designs for the purpose of measuring cell density in a bioreactor containing a mammalian culture.[8] Product information from one of the probe vendors presents experimental evidence that both scattering and absorbance can play a role in determining the signal in transmission-type cell density measurements.[10] The main point is that, regardless of the exact origin of the signal, the above data provide proof that absorbance/forward scatter can be used for cell density measurements in Bead Injection applications.

Intracellular H_2O_2 measurements combined with automated cell counting

The intracellular H_2O_2 response was measured using the protocol shown in Table 1. To reiterate, the protocol included loading a bead column and recording the absorbance signal, staining the cells with the H_2O_2 indicator DCFH-DA, and exposing the cells to H_2O_2 and measuring the ensuing fluorescence response. Fig. 5 illustrates typical data generated throughout the entire measurement cycle.

Normalization of signal to cell density. The observed fluorescence intensity is proportional to the number of cells in the detector field of view. Cell density information from the absorbance measurements can be used to normalize the signal, thus removing the proportional dependence. This is done by applying the formula

$$F_{\text{norm}} = \frac{F}{D}$$

where F_{norm} is the normalized fluorescence response, F is the raw response and D is the cell density (derived from the absorbance signal by using the calibration equation described above).

The normalization procedure was tested by measuring the intracellular response of cell populations seeded with 1×10^6, 2×10^6 and 4×10^6 cells exposed to 100 μM H_2O_2. Due to the different cell densities, the raw fluorescence responses of these populations are quite different as can be seen in Fig. 6 (black bars). The RSD of the three mean responses is high (47%), and analysis of variance (confidence level $\alpha = 0.05$) confirms that the responses differ to a statistically significant degree.

Normalization of the responses to cell density brings the responses closer to one another (RSD = 38%). However, the improvement is marginal and the responses remain distinctly different (Fig. 6, grey bars). Moreover, it is clear from Fig. 6 that the normalization has introduced a 'reverse bias' in the results, *i.e.* the response decreases with increasing cell density.

Correction for light intensity losses. The reverse bias observed in Fig. 6 (grey bars) can be explained by considering the factors influencing the observed fluorescence intensity. On the one hand, cells scatter and absorb some of the incoming light, causing attenuation of the excitation intensity:

$$I^{\text{ex}} = 10^{-l\_\text{ex}\cdot A} I_0^{\text{ex}}$$

where I^{ex} is the excitation intensity in the fiber field of view, I_0^{ex} is the incoming excitation intensity, l_ex is the effective path length (established by experiments with fluorescein described above) for excitation light and A is the observed absorbance.

On the other hand, the scattering/absorption also attenuates the fluorescence emission as the emitted light travels down through the column before reaching the collecting fiber:

$$F = 10^{-l\_\text{em}\cdot A} F_0$$

where F is the collected fluorescence intensity, F_0 is the original fluorescence emission intensity, l_em is the effective path length for emission light and A is the observed absorbance.

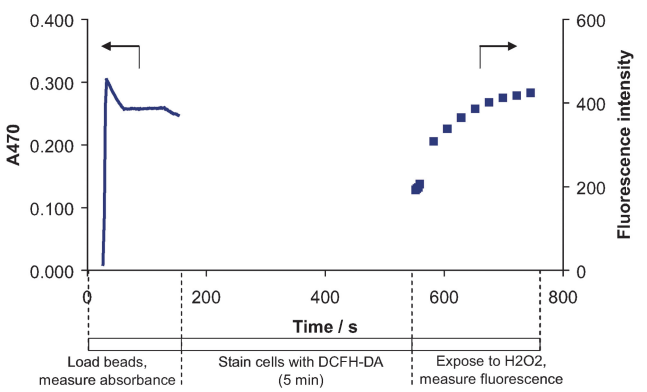

Fig. 5 Raw data resulting from one complete measurement cycle. The trace on the left is the absorbance signal. It shows an abrupt increase as the beads enter the flow cell, followed by a slight decrease as the colored culture medium is washed out. The trace on the right is the intracellular fluorescence signal, showing an increase upon exposure to H_2O_2.

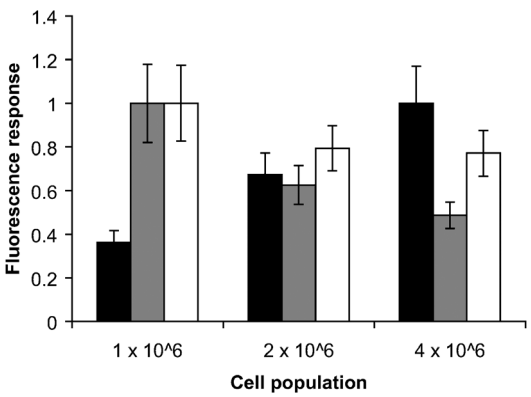

Fig. 6 Comparison of responses from different cell populations. Each population was exposed to 100 μM H_2O_2. The labels on the *x*-axis refer to the seeding densities of the populations. **Black bars**: responses in terms of raw fluorescence intensity (RSD 47%). **Grey bars**: responses after normalization to cell density (RSD 38%). **White bars**: responses after correction for light intensity (using l_ex = 0.50 and l_em = 0.50) and normalization to cell density (RSD 15%). The values were derived from four replicate measurements ($n = 4$). The responses have been scaled to a maximum relative value of 1.0 in order to permit displaying them in the same graph.

In summary, cell density influences the fluorescence signal in three different ways: (1) higher cell density translates into a larger amount of fluorescent indicator in the detector field of view; (2) higher cell density leads to decreased excitation intensity; and (3) higher cell density leads to decreased transmission of the emitted fluorescence. Consequently, three correction terms are needed:

$$F_{\text{norm}}^{\text{corr}} = \frac{F}{D \cdot 10^{-l\_\text{ex} \cdot A} \cdot 10^{-l\_\text{em} \cdot A}} = \frac{F}{D \cdot 10^{-(l\_\text{ex} + l\_\text{em}) \cdot A}}$$

where $F_{\text{norm}}^{\text{corr}}$ is the normalized and intensity-corrected fluorescence response, and F, D, l_ex, l_em and A are as defined above.

Full correction. When both normalization and intensity correction are applied to the H_2O_2 response data, the responses are significantly closer to one another (Fig. 6, white bars). It can be seen that the corrected response for the lowest cell density appears to differ somewhat from those of the two higher densities, although not quite in a statistically significant manner (based on analysis of variance, at confidence level $\alpha = 0.05$). This may be a sign that the intracellular peroxide response is slightly dependent on cell density, or it could reflect random responsivity differences between populations.

Examples of real-time fluorescence responses to different levels of H_2O_2 are shown in Fig. 7A. A plot of normalized and intensity-corrected responses to different H_2O_2 exposures is shown in Fig. 7B. The normalized dose response is non-linear; however, this is consistent with the cell biology, as intracellular antioxidant capacity is exceeded in the mid-range of the curve, and response is saturated by cellular toxicity at the high range of the curve (there is no further increase in normalized signal above 100 μM, data not shown).

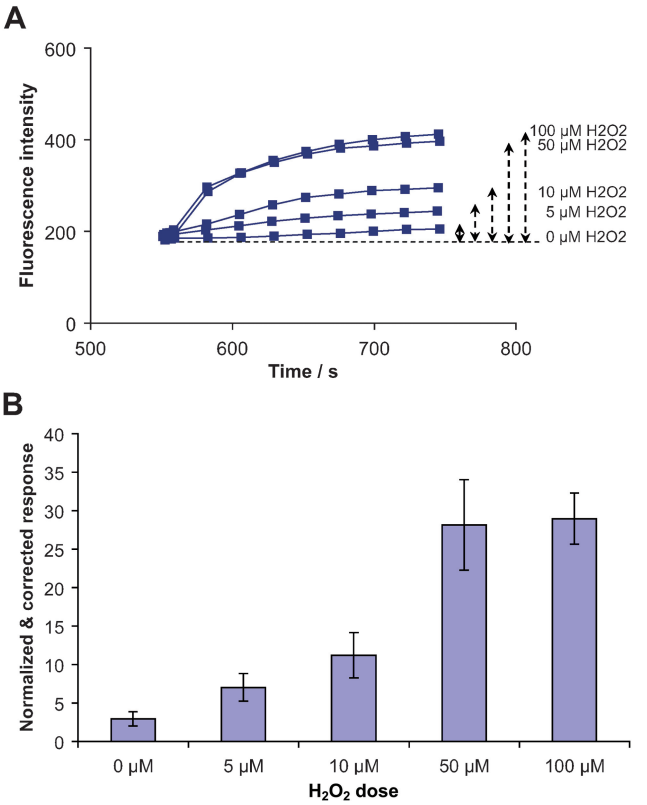

Fig. 7 (A) Intracellular H_2O_2 responses to different doses of H_2O_2 in the extracellular medium. The arrows indicate how the response signals were derived from the raw data. (B) Normalized and intensity-corrected signals from exposure to different levels of H_2O_2. The reported values are averages of four replicate measurements ($n = 4$).

Conclusions

The ability to normalize the fluorescence signal to cell density is necessary for accurate use of fluorescent indicators. Our approach to normalization avoids the time-consuming manual cell counting and the use of a microscope for both cell count and fluorescence monitoring. While native absorbance/forward scatter is not the most accurate measure of cell density, since both live and dead cells give rise to a signal, it is much faster and more convenient than any type of live/dead staining. It allows the density measurement to be carried out for every cell sample under investigation, since the cells are not exposed to a live/dead stain that could interfere with the H_2O_2 indicator.

For most fluorescent indicators, the prevalent practice is to stain the entire cell population before conducting experiments on them. We have taken a different approach in staining the cells with the H_2O_2 indicator on-line and one fraction at a time. This approach is advantageous for indicators like DCFH-DA that are prone to spontaneous oxidation and leaching out of cells.[6] On-line staining reduces such effects by minimizing the time between loading the indicator into cells and recording the response. Furthermore, since all the steps are automated, inconsistencies related to manual operations are eliminated. On-line staining also allows the absorbance signal to be measured before introducing the dye, thus avoiding absorbance artifacts due to the presence of the dye. Finally, since the staining, washing, and measurement steps are carried out immediately after one another, any cytotoxic effects of the indicator are minimized.

The Lab-on-valve concept, although of rather recent origin,[3] is now being widely recognized as documented by more than 100 papers and over 400 citations.[11] The present work adds a novel facet to this technology, by implementing simultaneous measurement of absorbance and fluorescence in the same flow cell. While this unique feature could undoubtedly have been implemented for conventional solution-phase measurements, we have chosen to demonstrate its potential in the more challenging Bead Injection format.

Bead Injection was originally developed to carry out fluorescent immunochemical measurements on a solid-phase substrate.[12,13] Later on, the use of BI was expanded to live cell measurements, namely to dynamic intracellular Ca^{2+} release studies, where live cells were exposed to gradients of biologically active agents.[14,15] Along similar lines, BI found application in monitoring cellular metabolic rates *via* acid accumulation or oxygen consumption.[16] These early BI applications offered a new way of performing dynamic ligand-binding and live-cell analyses, relying on the use of a fluorescence microscope as the detector. While a fluorescence microscope can be a sensitive detector, its high price and large size restricts the applicability of the BI technology in this format. The present approach eliminates these

drawbacks, making Bead Injection a much more attractive technique for live-cell studies.

Double spectrometry can be further exploited by using absorbance measurement not just in a supporting role, but for truly quantitative assays. This is not a far-fetched assumption, as our previous work on monitoring protein immobilization shows that absorbance monitoring of packed beads, in the same configuration as used in this work, allows the quantitative assay of captured proteins to be carried out.[17] Hopefully this work will inspire others to use double spectrometry in the LOV format to develop novel biochemical assays, not only in the BI format, but also for conventional solution-phase measurement, since the LOV flow cell described here can be used without any modifications for reagent-based assays or for post-column monitoring.[18]

Acknowledgements

The authors express their gratitude to the National Institutes of Health for support by Grant Number R01EB000782, awarded by the National Institute of Biomedical Imaging and Bioengineering and Grant P30 AG13280. The content is solely the responsibility of the authors and does not necessarily represent the official views of the National Institute of Biomedical Imaging and Bioengineering or the National Institutes of Health.

References

1 R. P. Haugland, *Handbook of Fluorescent Probes and Research Products*, Molecular Probes, Eugene, 9th edn, 2002.
2 Y. Umezawa, *Annu. Rev. Anal. Chem.*, 2008, **1**, 397–421.
3 J. Ruzicka, *Analyst*, 2000, **125**, 1053–1060.
4 M. D. Luque de Castro, J. Ruiz-Jiménez and J. A. Pérez-Serradilla, *Trends Anal. Chem.*, 2008, **27**, 118–126.
5 C. E. Lenehan, N. W. Barnett and S. W. Lewis, *Analyst*, 2002, **127**, 997–1020.
6 J. A. Royall and H. Ischiropoulos, *Arch. Biochem. Biophys.*, 1993, **302**, 348–355.
7 K. K. Sanford, W. R. Earle, V. J. Evans, H. K. Waltz and J. E. Shannon, *J. Natl. Cancer Inst.*, 1951, **11**, 773–795.
8 P. Wu, S. S. Ozturk, J. D. Blackie, J. C. Thrift, C. Figueroa and D. Naveh, *Biotechnol. Bioeng.*, 1995, **45**, 495–502.
9 W. L. Connors and J. Heino, *Anal. Biochem.*, 2005, **337**, 246–255.
10 *Cell Density Measurement Primer*, Finesse LLC, Santa Clara, CA, USA.
11 A literature search on the Web of Science on 13 May 2008.
12 C. H. Pollema and J. Ruzicka, *Anal. Chem.*, 1994, **66**, 1825–1831.
13 B. Willumsen, G. D. Christian and J. Ruzicka, *Anal. Chem.*, 1997, **69**, 3482–3489.
14 P. S. Hodder and J. Ruzicka, *Anal. Chem.*, 1999, **71**, 1160–1166.
15 P. S. Hodder, C. Beeson and J. Ruzicka, *Anal. Chem.*, 2000, **72**, 3109–3115.
16 I. Lähdesmäki, J. Ruzicka and A. Ivaska, *Analyst*, 2000, **125**, 1889–1895.
17 J. Ruzicka, A. D. Carroll and I. Lähdesmäki, *Analyst*, 2006, **131**, 799–808.
18 H. Erxleben and J. Ruzicka, *Analyst*, 2005, **130**, 469–471.

